

Collisional Narrowing of a Fine-Structure Raman Transition

S. Saoudi, Ch. Lermينياux, and M. Dumont

Laboratoire de Physique des Lasers, Université Paris-Nord, 93430 Villetaneuse, France

(Received 27 January 1986)

The line shape of the Raman transition between metastable levels of neon (3P_0 and 3P_2) is studied as a function of the pressure of a helium buffer gas. Dicke narrowing of the Doppler-broadened nonresonant Raman signal (for large optical detunings) gives the first evidence of conservation of a fine-structure coherence by velocity-changing collisions. Pressure broadening of the resonant Raman signal gives a measurement of the velocity-changing-collision rate.

PACS numbers: 32.70.Jz, 34.40.+n, 42.65.Dr

Velocity-changing collisions (VCC) have been widely studied with use of saturation-spectroscopy techniques.¹⁻⁵ In principle, saturation line shapes are sensitive to "population VCC" which conserve populations of molecular energy levels (elastic collisions) and to "coherence VCC" which preserve also quantum coherent superpositions of molecular states. Practically, the coherence VCC are difficult to study⁴: Only photon echoes,^{6,7} for small-angle scattering, and collisional-narrowing⁸⁻¹² (Dicke narrowing¹³) of Doppler-broadened lines, for large-angle scattering, have proved unambiguously the existence of coherence VCC.

Conservation of coherence by large-angle-scattering VCC has interesting consequences regarding the intermolecular potentials giving rise to this scattering. As Berman¹ has pointed out, the intermolecular potentials must be parallel for levels involved in the linear superposition. This situation is unlikely for electronic transitions, but exists for atomic hyperfine and Zeeman structures and for molecular vibrational and rotational transitions: This has been proved by the collisional narrowing of some lines in microwave⁸ or infrared spectra,⁹ in spontaneous¹⁰ or stimulated¹¹ Raman spectra, and in four-wave mixing experiments.¹²

In this paper we present what, to our knowledge, is the first observation of conservation of a fine-structure coherence by large-angle-scattering VCC. The existence of this conservation was not obvious as it implies that interatomic potentials are not sensitive to spin-orbit coupling. We have used the stimulated Raman effect between the two metastable levels of neon, 3P_0 and 3P_2 , in the presence of a He buffer gas.

Let us consider a three-level system [Fig. 1(a)], a saturating beam (ω_s, k_s) almost resonant with transition $a-c$ (detuning $\delta_s = \omega_s - \omega_{ac}$), and a copropagating probe beam (ω_p, k_p) almost resonant with transition $a-b$ ($\delta_p = \omega_p - \omega_{ab}$). Variations of probe-beam absorption induced by a low-intensity saturating beam are easily calculated with a third-order perturbation development of the density matrix¹⁴. Considering only the terms which involve the Raman coherence

($\sigma_{bc}^{(2)}$) at the second order and neglecting VCC, for the moment, one obtains the well-known result

$$\mathcal{I} \propto \text{Re} \int \left[\frac{N_b}{L_{ab}^2} + \frac{N_c}{L_{ab}L_{ac}^*} \right] \frac{W(v)}{L_{bc}} dv, \quad (1)$$

where $W(v) \propto \exp[-(v^2/u^2)]$ is the Maxwell velocity distribution, N_b and N_c are the total populations of levels b and c (assuming $N_a=0$), and L_{ij} are the energy denominators in which Γ_{ij} is the relaxation rate for coherence σ_{ij} , including radiative relaxation [$\frac{1}{2}(\gamma_i + \gamma_j)$] and dephasing collisions (Γ_{ij}^{ph}):

$$L_{ab} = \Gamma_{ab} + i(\delta_p - k_p v), \quad L_{ac} = \Gamma_{ac} + i(\delta_s - k_s v), \\ L_{bc} = \Gamma_{bc} + i[\delta_p - \delta_s - (k_p - k_s)v].$$

Usually, expression (1) is calculated analytically in two extreme cases. The first one is the "resonant Raman signal" (RRS) obtained for small detunings ($\delta_s \leq k_s u$), when all L_{ij} are resonant for the same velocity group. It is a sharp peak centered at $\delta_p = \delta_s k_p / k_s$. At the Doppler limit [$W(v)$ much broader than all L_{ij}^{-1}], for $0 < k_s < k_p$, its width is¹⁵

$$\Gamma_N = \Gamma_{bc} + \Gamma_{ac} (k_p - k_s) / k_s.$$

The RRS is due to a single velocity group selected by the saturating beam: It is a homogeneous line.

The second case is the nonresonant Raman signal (NRRS) obtained at large detuning ($\delta_s \gg k_s u$), which constitutes the usual Raman signal. Only L_{bc}

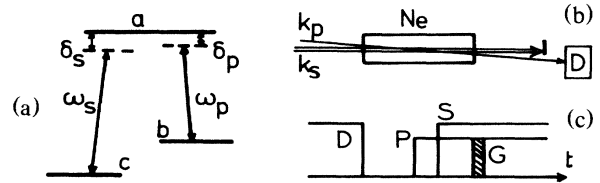


FIG. 1. (a) Energy levels and laser frequencies. (b) Experimental geometry. (c) Time diagram of experimental pulses (D = discharge, S = saturating beam, P = probe beam, and G = signal integration gate).

can be resonant, while $L_{ab} \approx i\delta_p$ and $L_{ac} \approx i\delta_s$:

$$\mathcal{S}_{NR} \approx \left[\frac{N_c}{\delta_s \delta_p} - \frac{N_b}{\delta_p^2} \right] \text{Re} \int \frac{W(v)}{L_{bc}} dv. \quad (2)$$

This is a Voigt profile centered at $\delta_p = \delta_s$. At the Doppler limit it reduces to a Gaussian function of half-width $|k_p - k_s|u$, which directly reflects the atomic velocity distribution: The NRRS is an inhomogeneous line.

Let us consider VCC conserving the Raman coherence σ_{bc} and characterized by a rate Γ_{bc}^{vc} and an average velocity change Δv . At low pressure, as long as $|k_s - k_p|\Delta v$ is much greater than the homogeneous width Γ_{bc} , any VCC will remove atoms from the velocity group contributing to the Raman signal. One has simply to include VCC in the total relaxation rate:

$$\Gamma_{bc} = \Gamma_{bc}^{vc} + \Gamma'_{bc}, \quad \Gamma'_{bc} = \frac{1}{2}(\gamma_b + \gamma_c) + \Gamma_{bc}^{ph}. \quad (3)$$

Therefore, the RRS broadens linearly with pressure (its amplitude decreases as $\Gamma_N^{-1}\Gamma_B^{-1}$),¹⁵ while the NRRS is unaffected since its line shape (2) is mainly Gaussian.

At higher pressure, when $\Gamma_{bc} \geq |k_p - k_s|\Delta v$, atoms continue to interact coherently with the laser beams after a VCC. The equation for Raman coherence $\sigma_{bc}^{(2)}(v)$ becomes a Boltzmann equation with a collision kernel coupling all velocities.^{1,6} The RRS no longer broadens linearly with pressure, but its amplitude is very small. Finally, when $\Gamma_{bc} \gg |k_p - k_s|u \gg \Gamma'_{bc}$, the NRRS exhibits Dicke narrowing. Indeed the atomic velocity (and therefore the Doppler phase shift) has no time to build up between two successive collisions (mean time $1/\Gamma_{bc}^{vc}$). The Doppler broadening disappears and the line becomes homogeneous. Its half-width Γ'_{bc} is the inverse of the coherence lifetime.

Experimentally, the NRRS has been studied for the Ne metastable levels with use of two cw dye lasers tuned near the lines $\lambda = 588.2$ nm [$1s_5(^3P_2)-2p_2$] and $\lambda = 616.3$ nm [$1s_3(^3P_0)-2p_2$]. Both lasers are linearly polarized in order to produce Raman coherence between the 3P_2 , $m=0$ sublevel and the 3P_0 level. The frequency of each laser is stabilized on a saturated-absorption signal scanned magnetically. This reproducible scanning allows signal integration over several frequency sweeps, but reduces the tuning range to a few gigahertz. To increase detuning on both lines, laser frequencies are locked on ^{22}Ne , while the experimental cell is filled with ^{20}Ne . Maximum detuning is 4.5 GHz.

Metastable levels are created by a rf discharge (210 MHz) in a tube 4 mm in diameter. As a result of the high power needed (~ 1 kW) for producing a discharge at high pressure (up to 160 Torr) the rf discharge is pulsed (~ 4 μsec ; repetition rate 1 kHz).

Measurements are performed in the afterglow regime, when main plasma effects are damped. After a few microseconds, the 3P_2 level is much more populated than the 3P_0 .¹⁶ The 3P_0 population can be neglected.

The saturating beam and probe beam are modulated by acousto-optic modulators [Fig. 1(c)]. Probe intensity is monitored by a gated integrator (boxcar), 2 μsec after the onset of the saturating beam. For this time delay, all coherent transients¹⁷ are damped, but optical pumping is not yet important. Indeed, even for $\delta_s \sim 5k_s u$, the saturating beam (30 mW; diameter ~ 0.5 mm) is able to progressively depopulate the lower level c . A part of this population is accumulated in level b , through spontaneous emission from level a : This produces a strong saturation signal in competition with the Raman signal.

Experiments have been performed with a constant partial pressure of ^{20}Ne (0.5 Torr) and partial pressures of He from 0 to 160 Torr. At higher pressures, it was impossible to produce a discharge. Figure 2(a) shows a set of experimental curves obtained with the saturating beam tuned 4.5 GHz from the center of the 588.2-nm line. In this case, referring to Fig. 1(a), $b = ^3P_0$ and $c = ^3P_2$. Therefore $N_b \ll N_c$: The Raman signal corresponds to probe amplification. Figure 2(a) clearly shows Dicke narrowing for pressures higher than 20 Torr. At low pressure the line shape is Gaussian while at high pressure the slowly decreasing wings are characteristic of a Lorentzian behavior. Figure 2(b) shows experimental curves obtained by choosing the saturating wavelength near the 616.3-nm line ($b = ^3P_2$; $c = ^3P_0$; $N_b \gg N_c$). Dicke narrowing is again evident in spite of a greater asymmetry. Figure 3 shows the NRRS width as a function of He pressure.

To measure the total collision rate, we have studied the RRS at low pressure (20 mTorr Ne; 0 to 1.5 Torr He) with a larger cell and a low-intensity rf discharge,¹⁷ in the configuration $0 < k_s < k_p$. Γ_{bc} is obtained from Γ_N with the use of experimental values for Γ_{ac} (4.5 MHz + 9.3 MHz/Torr, from the linear-absorption line shape). The pressure broadening is linear and leads to $\Delta\Gamma_{bc} = 4.8 \pm 0.5$ MHz/Torr of He. Over the pressure range ($P < 1.5$ Torr) where the signal was appreciable, there was no evidence for any nonlinear dependence of Γ_{bc} with pressure.

For comparison with experiments, the density matrix equations have been solved with VCC for Raman coherence only; optical coherences are supposed to be destroyed by VCC. Since the exact collision kernel [$A(v' \rightarrow v)$, the probability per unit of time that a single VCC changes the velocity from v' to v] is unknown and since the Boltzmann equation has no analytic solution in the general case, we have restricted the calculation to the "strong" collision model [$A(v' \rightarrow v) = \Gamma_{bc}^{vc} W(v)$] for which the velocity is completely thermalized by a single VCC. For any δ_s , the general solu-

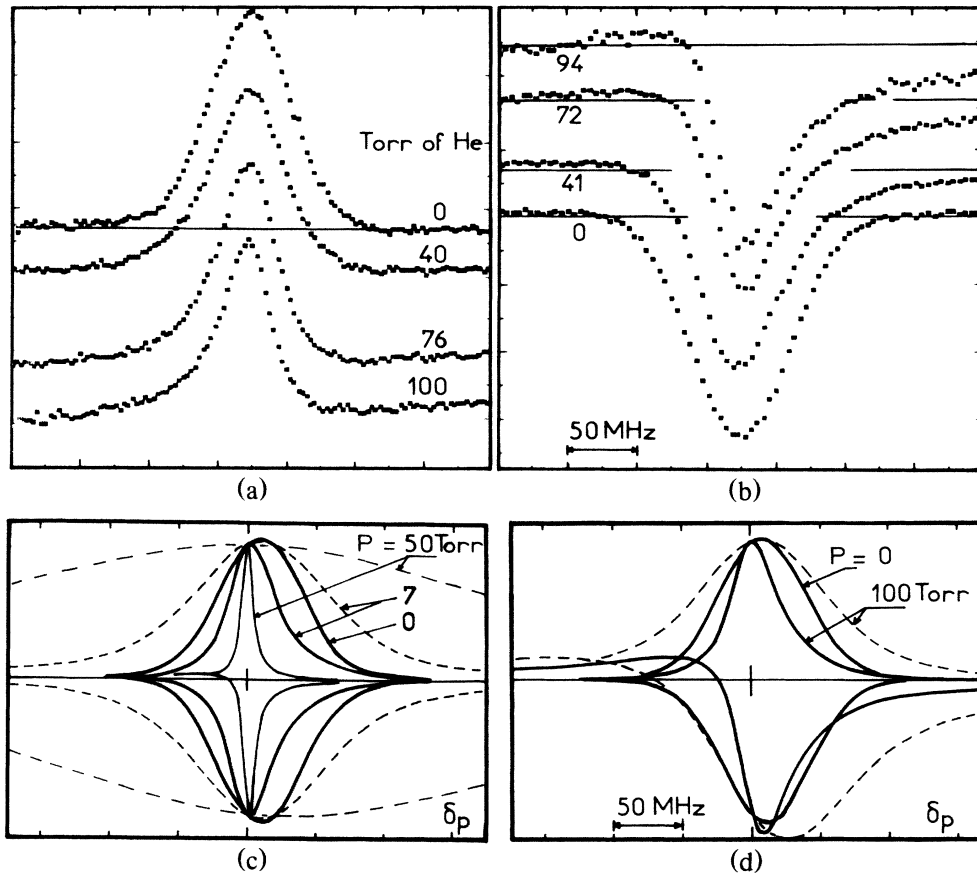


FIG. 2. NRRS line shape as a function of pressure. Upward-peaked curves (probe amplification) correspond to $N_b = 0$; downward ones, to $N_c = 0$. (a) Experimental curves with $\lambda_s = 588$ nm, $\lambda_p = 616$ nm, and $\delta_s = 4.5$ GHz. In this case $k_s > k_p$ and $N_c \gg N_b$. Since the lower level of the saturating beam ($c = {}^3P_2$) is populated, the optical pumping (from 3P_2 to 3P_0) rapidly increases with pressure and induces absorption of the probe; it appears as an increasing background. (b) Experimental curves with $\lambda_s = 616$ nm, $\lambda_p = 588$ nm, and $\delta_s = 4$ GHz. One has $k_s < k_p$ and $N_b \gg N_c$. NRRS is more asymmetric and there is no optical pumping ($N_c \approx 0$). (c) Theoretical line shape from the strong-collision model. $\delta_s = 4$ GHz; $\Gamma_{ab} = \Gamma_{ac} = 4.5$ MHz/Torr; $\Gamma_{bc}^{vc} = 4.8$ MHz/Torr; $\Gamma_{bc}^{ph} = 1$ MHz (for simulating the laser frequency jitter); $k_{su} = 887$ MHz; and $k_{pu} = 930$ MHz ($T = 360$ K from experimental Doppler width at 10 Torr). For the dashed curves, VCC have been replaced by dephasing collisions. All curves are normalized for $\delta_p = \delta_s$ (at the center of the graph). (d) Like (c), except $\Gamma_{bc}^{vc} = 0.3$ MHz/Torr. Relative to Γ_{bc} , Γ_{ab} and Γ_{ac} increase faster than in (a); therefore the asymmetry is greater.

tion is

$$\mathcal{I} \propto \text{Re} \left\{ \int \left[\frac{N_b}{L_{ab}} + \frac{N_c}{L_{ac}^*} \right] \frac{W(v)}{L_{ab}L_{bc}} dv + \Gamma_{bc}^{vc} \int \frac{W(v)}{L_{ab}L_{bc}} dv \int \left[\frac{N_b}{L_{ab}} + \frac{N_c}{L_{ac}^*} \right] \frac{W(v)}{L_{bc}} dv \left[1 - \Gamma_{bc}^{vc} \int \frac{W(v)}{L_{bc}} dv \right]^{-1} \right\}. \quad (4)$$

Assuming that the RRS broadening is due to VCC only, we have calculated the theoretical NRRS line shape with $\Gamma_{bc}^{vc} = 4.8$ MHz. As shown by Fig. 2(c) and curve A of Fig. 3, the Dicke narrowing is much faster than the experimental one. Any attempt to introduce partially dephasing collisions ($\Gamma_{bc}^{ph} + \Gamma_{bc}^{vc} = 4.8$ MHz/Torr) leads to unacceptable theoretical curves. Considering the mass ratio of Ne to He, this result is not surprising, since the collision kernel is expected to be much narrower than a strong-collision kernel.¹⁸ The

thermalization of the Ne velocity necessitates several collisions with He. For that reason we tried effective values for Γ_{bc}^{vc} in expression (3). As shown in Fig. 2(d) and Fig. 3, a very good agreement with experimental results is obtained at high pressure, for $(\Gamma_{bc}^{vc})_{\text{eff}} = 0.3$ MHz/Torr. From a statistical point of view, sixteen He-Ne collisions are equivalent to one strong collision for thermalization of the Ne velocity. In spite of the oversimplification of the theoretical

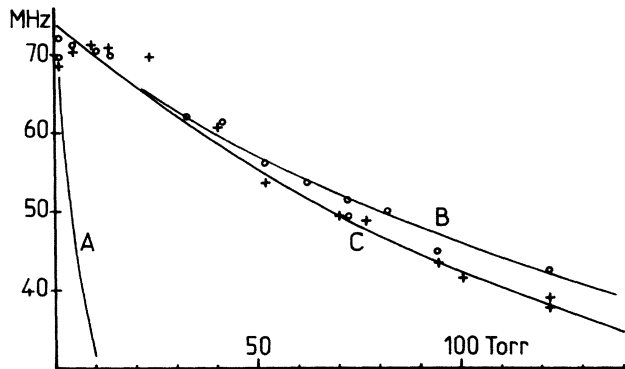


FIG. 3. Experimental NRRS full width at half height vs pressure of helium. Crosses, $\delta_s = 4.5$ GHz, $\lambda_s = 588$ nm, $\lambda_p = 616$ nm. Circles, $\delta_s = 4$ GHz, $\lambda_s = 616$ nm, $\lambda_p = 588$ nm. The theoretical curves correspond to (a) $k_p > k_s$, $\delta_s = 4$ GHz, N_c or $N_b = 0$, $\Gamma_{bc}^{yc} = 4.8$ MHz/Torr; (b) $k_p > k_s$, $\delta_s = 4$ GHz, $N_c = 0$, $\Gamma_{bc}^{yc} = 0.3$ MHz/Torr (like circles); (c) $k_s > k_p$, $\delta_s = 4.5$ GHz, $N_b = 0$, $\Gamma_{bc}^{yc} = 0.3$ MHz/Torr (like crosses). Other parameters are the same as in Fig. 2. The discrepancy at low pressure is due to the theoretical model but also to temperature variations (the power of the discharge is reduced).

model, the line-shape asymmetry is in excellent agreement with experimental observations. Asymmetry is due to the fact that the detuning δ_s is not much larger than $k_s u$ and than Γ_{ab} and Γ_{ac} at high pressures.

We have shown that elastic collisions with helium do not destroy coherent superpositions of 3P_0 and 3P_2 metastable levels of neon ($\Gamma_{bc}^{ph} \approx 0$). This result, which was not obvious, leads to the conclusion that the corresponding interatomic potentials are insensitive to spin-orbit coupling. Model potential calculations¹⁹ seem to support this conclusion. Cross-beam experiments have been undertaken to measure differential cross sections directly.

We are very grateful to P. R. Berman for suggesting this experiment to us and for valuable discussions.

¹P. R. Berman, Appl. Phys. **6**, 283 (1975); see also other references in this paper.

²P. R. Berman, P. F. Liao, and J. E. Bjorkolm, Phys. Rev. A **20**, 2389 (1979).

³S. G. Rautian and I. I. Sobel'man, Usp. Fiz. Nauk. **90**, 209 (1967) [Sov. Phys. Usp. **9**, 701 (1967)]; S. G. Rautian, Zh. Eksp. Teor. Fiz. **51**, 1176 (1966) [Sov. Phys. JETP **24**, 788 (1967)].

⁴J. L. Le Gouët and P. R. Berman, Phys. Rev. A **17**, 52 (1978). In this reference, the resonant Raman signal is calculated for small-angle-scattering coherence VCC. The theoretical line shape is modified, but experimentally it is not easily distinguishable from a small modification of Γ_{bc} in the collisionless formula [Ph. Cahuzac, J. L. Le Gouët, P. E. Toschek, and R. Vetter, Appl. Phys. **20**, 83 (1979)].

⁵M. Gorlicki, Ch. Lermniaux, and M. Dumont, Phys. Rev. Lett. **49**, 1394 (1982).

⁶P. R. Berman, T. W. Mossberg, and S. R. Hartmann, Phys. Rev. A **25**, 2550 (1982).

⁷T. W. Mossberg, R. Kachru, and S. R. Hartmann, Phys. Rev. Lett. **44**, 73 (1980); R. Kachru, T. J. Chen, S. R. Hartmann, T. W. Mossberg, and P. R. Berman, Phys. Rev. Lett. **47**, 902 (1981); R. A. Forber, L. Spinelli, J. E. Thomas, and M. S. Feld, Phys. Rev. Lett. **50**, 331 (1983).

⁸J. P. Wittke and R. H. Dicke, Phys. Rev. **103**, 620 (1956).

⁹N. M. Lawandy and G. A. Koepf, IEEE J. Quantum Electron **18**, 1054 (1982).

¹⁰J. R. Murray and A. Javan, J. Mol. Spectrosc. **42**, 1 (1972).

¹¹P. Lallemand, P. Simova, and G. Bret, Phys. Rev. Lett. **17**, 1239 (1966).

¹²I. J. Rothberg and N. Bloembergen, Phys. Rev. A **30**, 820 (1984).

¹³R. H. Dicke, Phys. Rev. **89**, 472 (1953).

¹⁴Th. Hänsch and T. Toschek, Z. Phys. **236**, 213 (1970).

¹⁵The RRS cancels for $k_s < 0 < k_p$. For $0 < k_s < k_p$, it consists of the difference between a narrow Lorentzian curve (width Γ_N) and a broad one [width $\Gamma_B = (k_s \Gamma_{ab} + k_p \Gamma_{ac}) / k_s$]. For $0 < k_p < k_s$, the RRS is more complicated [Hansch and Toschek, Ref. 14, and Ch. Lermniaux and M. Dumont, J. Opt. Soc. Am. B (to be published)].

¹⁶C. O. Akoshile, J. D. Clark, and A. J. Cunningham, J. Phys. B **18**, 2793 (1985).

¹⁷Lermniaux and Dumont, Ref. 15.

¹⁸This is confirmed by experimental observation of the He-Ne(3P_0) population kernel (unpublished), with the method described in Ref. 5.

¹⁹P. E. Siska, J. Chem. Phys. **73**, 2372 (1980); D. Hennecart and F. Masnou-Seeuws, J. Phys. B **18**, 657 (1985).